Environmental Science & Technology

Article

pubs.acs.org/est

Time-Resolved Characterization of Primary Emissions from Residential Wood Combustion Appliances

M. F. Heringa,[†] P. F. DeCarlo,[†,⊥] R. Chirico,[†,#] A. Lauber,[‡] A. Doberer,[‡,¶] J. Good,[‡] T. Nussbaumer,[‡] A. Keller,[§] H. Burtscher,[§] A. Richard,[†,▲] B. Miljevic,[∥] A. S. H. Prevot,[†,*] and U. Baltensperger[†]

[†]Laboratory of Atmospheric Chemistry, Paul Scherrer Institute, 5232 Villigen PSI, Switzerland

[‡]Lucerne University of Applied Sciences and Arts, 6002 Luzern, Switzerland

[§]Institute for Aerosol and Sensor Technology, University of Applied Sciences, Northwestern Switzerland, 5210 Windisch, Switzerland

[∥]International Laboratory for Air Quality and Health, Queensland University of Technology, Brisbane, Queensland 4001, Australia

Supporting Information

ABSTRACT: Primary emissions from a log wood burner and a pellet boiler were characterized by online measurements of the organic aerosol (OA) using a high-resolution time-of-flight aerosol mass spectrometer (HR-TOF-AMS) and of black carbon (BC). The OA and BC concentrations measured during the burning cycle of the log wood burner, batch wise fueled with wood logs, were highly variable and generally dominated by BC. The emissions of the pellet burner had, besides inorganic material, a high fraction of OA and a minor contribution of BC. However, during artificially induced poor burning BC was the dominating species with ~80% of the measured mass. The elemental O:C ratio of the OA was generally found in the range of 0.2−0.5 during the startup phase or after reloading of the log wood burner. During the burnout or smoldering phase, O:C ratios increased up to 1.6−1.7, which is similar to the ratios found for the pellet boiler during stable burning conditions and higher than the O:C ratios observed for highly aged ambient OA. The organic emissions of both burners have a very similar H:C ratio at a given O:C ratio and therefore fall on the same line in the Van Krevelen diagram.

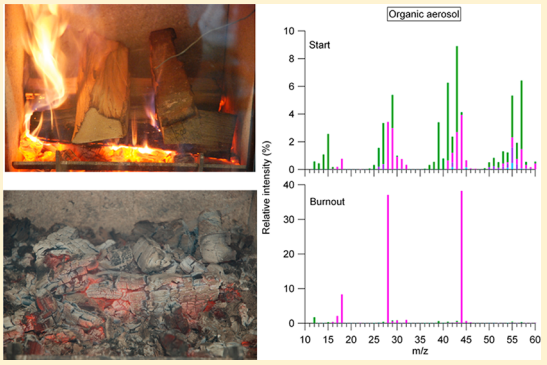

1. INTRODUCTION

Organic aerosols (OA) from domestic wood combustion can have an important contribution to the ambient concentration of PM_1 (particulate matter with an aerodynamic diameter $d_a < 1$ μm) in residential areas. During winter time, wood-burning emissions were found to be an important source of PM_1, often more important than traffic for organic aerosols, in Switzerland[1] and the dominant PM_1 source in Swiss Alpine valleys.[2,3] In summer, wood-burning and biomass-burning related emissions originating from outdoor fireplaces or forest fires can have major impacts on ambient PM levels.

Log wood burners emit a wide range of volatile organic compounds (VOCs), semivolatile organic compounds (SVOCs), and PM consisting mainly of OA and black carbon (BC).[4,5] These emissions, including the OA composition, depend on burner and wood type as well as the burning conditions.[6−8] The VOCs emitted by these burners can undergo oxidation reactions and form secondary organic aerosol (SOA), leading to enhanced PM concentrations.[9,10] Automated pellet burners, due to their high efficiency, produce less OA and BC, leaving inorganic compounds like potassium salts as the dominant fraction of the PM.[11] In addition, less gas phase hydrocarbons are emitted, leading to much lower SOA formation compared to that of a log wood stove.[10]

Short-term exposure to high PM concentrations influences human well-being.[12] Long-term exposure to moderate concentrations has been associated with increased mortality [13] and an increased risk of lung cancer.[14] Besides the mere quantity, adverse health effects also depend on the OA properties. Reactive oxygen species (ROS), likely to produce oxidative stress at the cellular level, were found in the emissions from a log wood burner whereas no ROS were found in the emissions from a pellet boiler.[15] Wood-burning emissions are highly variable in quantity and properties. This makes highly time-resolved online analysis essential for a detailed characterization of the aerosol emissions throughout the different burning phases. Online measurements have, besides the high time resolution, the advantage that positive (adsorption of gaseous compounds) or negative artifacts (volatilization of semivolatile material) on filters can be avoided.

With the increased awareness of the importance of renewable energy, wood burning has the potential to become a more abundant source of energy. Therefore, a detailed character-

Received: May 3, 2012
Revised: August 30, 2012
Accepted: September 12, 2012
Published: September 12, 2012

dx.doi.org/10.1021/es301654w | Environ. Sci. Technol. 2012, 46, 11418−11425

ization of the emissions from residential heating systems is of key importance for models to predict the impact on local and regional PM concentrations and for legal authorities as a basis for future legislation.

In this study, we characterized the emissions of an automated pellet boiler and a residential log wood burner. The evolution of the OA and BC concentrations were measured at a 10 s time resolution with an Aerodyne high-resolution time-of-flight aerosol mass spectrometer (HR-TOF-AMS) and a multi-angle absorption photometer (MAAP), respectively. This revealed that rapid fluctuations in OA concentration and its elemental composition occur during different burning conditions. The sum of the PM concentrations measured by the AMS and MAAP was compared to measurements by a tapered element oscillating microbalance (TEOM) for the determination of the fraction of refractory inorganic compounds. On the basis of high-resolution AMS spectra, the OA was characterized and compared to the characteristics of ambient OA.

2. EXPERIMENTAL SECTION

2.1. Wood-Burning Appliances and Sampling Setup. A series of wood-burning experiments were performed with a log wood burner and a pellet boiler at the wood burner test facility of the Lucerne University of Applied Sciences and Arts.[16] The log wood burner (Carena, Tiba, Switzerland), typically used for domestic heating, had a nominal power output of 8 kW and was fired with beech logs (moisture content ~20%). For a typical batchwise burning cycle of approximately 4 hours, the first batch (2−3 kg) was ignited from the top using small pieces of wood. After the burnout, the fire was restarted by adding ~3 kg of wood followed by two standard batches of 2−3 kg, which were added on top of the glow bed. This top-down burning procedure during the cold start reduces the PM emissions for the first batch by 50−80% compared to the traditional bottom-up start.[17]

The pellet boiler (LPK 15, Liebi, Switzerland), typically used for heating apartment buildings, was a 15 kW boiler automatically operated using wood pellets (8 × 15 mm, moisture content 6.8%). Pellets were added automatically at a rate of ~4.4 kg/h. The pellet boiler was equipped with a controlled two-stage air system injecting a primary airflow to the fuel bed and a secondary airflow to the combustion chamber. A typical test run consisted of a cold start and a stable burning period (air to fuel ratio (λ) 1.5−1.6), followed by a warm restart. In addition, to simulate nonoptimal conditions that could be the result of lack of maintenance or operational errors, poor burning conditions induced by restricting the air intake were tested at λ 1.2−1.3.

Both appliances were running at a test rig connected to a 150 mm diameter chimney equipped with a controlled draft system operated at 12 Pa as described in the European type test (EN303-5). Emissions were sampled from the chimney through a PM_{10} cyclone using a two-stage ejector dilution system (VKL 10, Palas, Germany). The sampling line, cyclone, and first dilution stage (factor ~17) was operated at 150 °C to prevent condensation of SVOCs. The second dilution stage (factor ~17) was operated at room temperature to enable online sampling at room temperature. Actual dilution factors were determined during the burning experiments by CO_2 measurements sampled directly from the chimney and after dilution and were in the range of 293−350, close to the expected factor of 289. A schematic representation of the setup is shown in Figure 1.

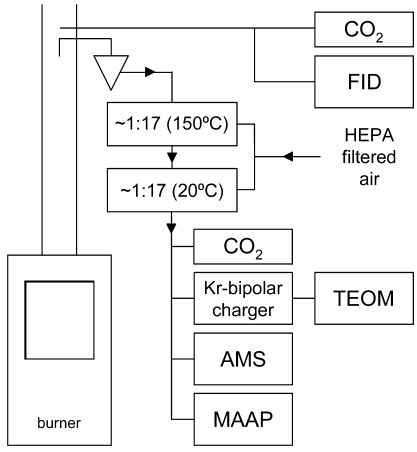

Figure 1. Schematic representation of the sampling system.

2.2. Instrumentation. An HR-TOF-AMS[18] was used for the online characterization and quantification of the submicrometer nonrefractory aerosol components, that is, species that evaporate rapidly at 600 °C and 10^{-7} Torr.[19] These species include OA (Org), nitrate (NO_3), sulphate (SO_4), ammonium (NH_4) and chloride (Chl). The high mass resolution and accuracy made it possible to determine the elemental composition of the ions,[18] and elemental ratios like O:C and H:C as well as the ratio of the organic matter to organic carbon (OM:OC).[20,21] On the basis of their elemental composition, ions were grouped into four different families: C_xH_y ($x \geq 1$ and $y \geq 0$), $C_xH_yO_z$, $C_xH_yN_p$ and $C_xH_yO_zN_p$ ($x \geq 1$, $y \geq 0$, $z \geq 1$, and $p \geq 1$) which will be referred to as CH, CHO, CHN, and CHON families from here on. The AMS was operated with a time resolution of 10 s to 1 min depending on burner type and burning conditions. Data analysis was performed using Igor Pro 6 (Wavemetrics, Lake Oswego, OR) with the Squirrel TOF analysis tool kit v1.51B and the Pika TOF HR analysis tool kit v1.10B. A dynamic gas phase CO_2 correction was applied to the AMS fragmentation table.[19] A CE of 1 was found based on the comparison of the sum of the AMS species and BC with a TEOM (Series 1400a, Thermo Scientific) operated at 50 °C and a time resolution of 10 s. The MAAP (Model 5012, Thermo Fisher Scientific) was used to determine BC based on the light absorption at 630 nm using a mass specific absorption cross section of 6.6 m^2/g.[22] The MAAP was operated at a time resolution of 1 s. Carbon dioxide (CO_2) and gas phase hydrocarbons (HC) were measured at a 1 s time resolution using a differential, nondispersive, infrared (NDIR) gas analyzer (LI-7000, Li-Cor Biosciences) and a flame ionization detector (FID) operated at 180 °C, respectively. The pellet burner setup was equipped with a VE7, JUM engineering FID, and the log wood burner setup with the Hartmann & Braun FIDAS 3E.

3. RESULTS AND DISCUSSION

3.1. Particle Measurements. The PM emissions of log wood burners are dominated by OA and BC [23] while automated furnaces and pellet burners due to their more complete combustion emit less OA and contain large fractions of inorganic compounds like potassium salts.[10] Figure 2 shows the concentration (corrected for dilution) measured by the TEOM (PM_{10}), versus the sum of the concentrations measured

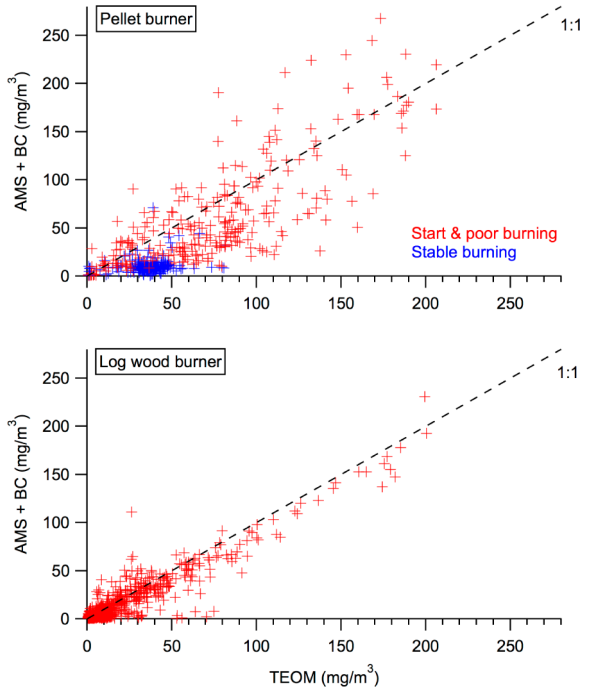

Figure 2. Comparison of the sum of the AMS species and BC vs TEOM. The pellet burner data (top panel) is separated in stable burning conditions (in blue) and the startup and poor burning conditions (in red).

by the AMS and the MAAP for a typical test cycle of the pellet burner and the log wood burner. The pellet burner data is scattered around the 1:1 line for the data points taken during the startup and the induced poor burning period indicating that during these phases the emissions are dominated by the nonrefractory components measured by the AMS and BC and have a particle size in the PM_1 range. However, during the stable burning phase only 32% of the concentration measured by the TEOM could be attributed to the sum of the AMS species and BC indicating a dominant contribution of inorganic salts during stable combustion. Even if the CE were lowered by the high salt fraction, e.g., to 0.5, the AMS species would contribute only up to 48% of the total mass. During these stable burning conditions, a diffusion size classifier (DiSC, home-built, see ref 24) measured a number-based mean particle diameter of 100 nm, which is ~30 nm less compared to the poor burning test and well within the range observed for the log wood burner. Therefore, assuming no increase in coarse particles during stable burning compared to the startup phase and poor burning conditions, the deviation from the 1:1 line during stable burning cannot be explained by the size cut of the individual instruments. The log wood data follows closely the 1:1 relation, which confirms the small contribution of inorganic salts to the PM emissions from log wood burners and therefore the sum of the AMS species and BC is a representative measure of PM from the log wood burner tested here. PM emissions as a function of energy output and averaged emission factors for both burners and the different burning conditions are shown in the Supporting Information.

3.2. Emission Composition. The concentrations (corrected for dilution) of the AMS species, BC, and HCs for a typical experiment cycle of the pellet burner and log wood burner are shown in Figure 3. The emissions of the pellet burner showed several peaks in OA and BC concentration during the first ~15 min of the cold start before it reached the stable burning phase where the concentrations were constant at a relatively low level. The warm restart resulted again in a short spike in the OA concentration, which was about a factor of 2 lower compared to the cold start and shorter in duration. During the poor burning test phase the concentrations of OA and BC increased and showed rapid and large fluctuations, likely the result of short periods of (local) lack of oxygen. Modified combustion efficiencies (MCE), defined as $[CO_2]/([CO_2] + [CO])$ were 0.999 and ~0.988 during stable burning and poor burning conditions, respectively. During stable burning the OA was the dominant carbonaceous species whereas the poor burning phase was dominated by BC. After

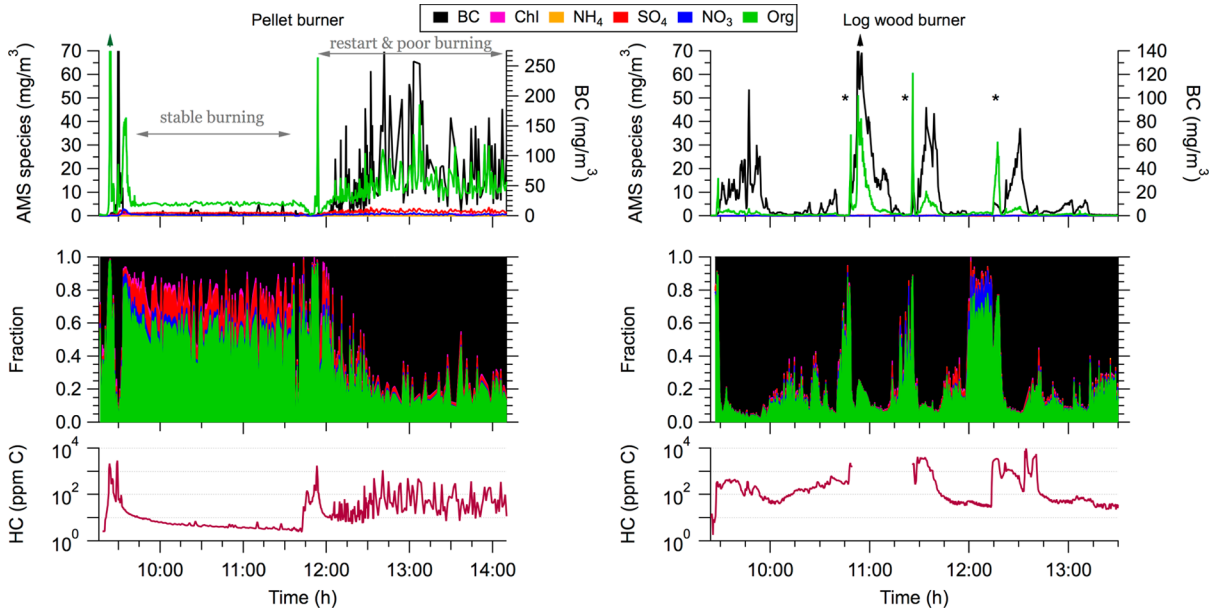

Figure 3. Temporal evolution of the AMS species and BC (top panel), their relative contributions (middle), and the HC concentration as ppm carbon (lower panel). The stars indicate the addition of wood logs to the fire. Concentrations are corrected for dilution.

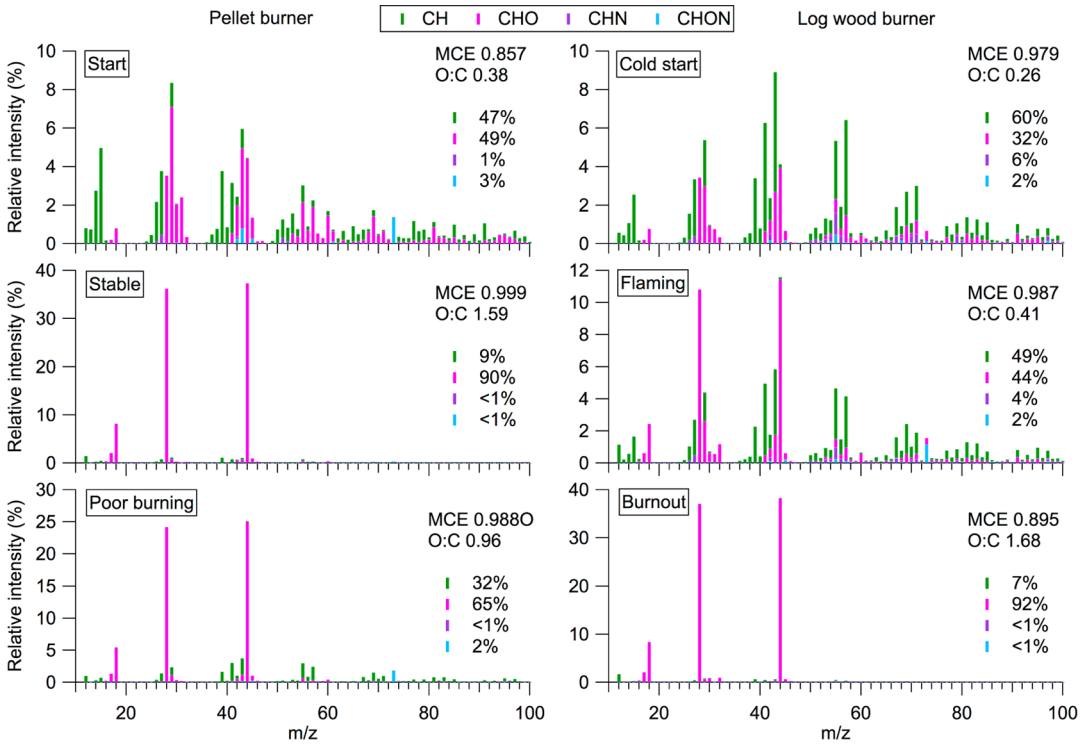

Figure 4. Comparison of the normalized high-resolution family mass spectra during different burning conditions. The numbers indicate the contributions of the CH, CHO, CHN, and CHON families to the organic mass spectrum.

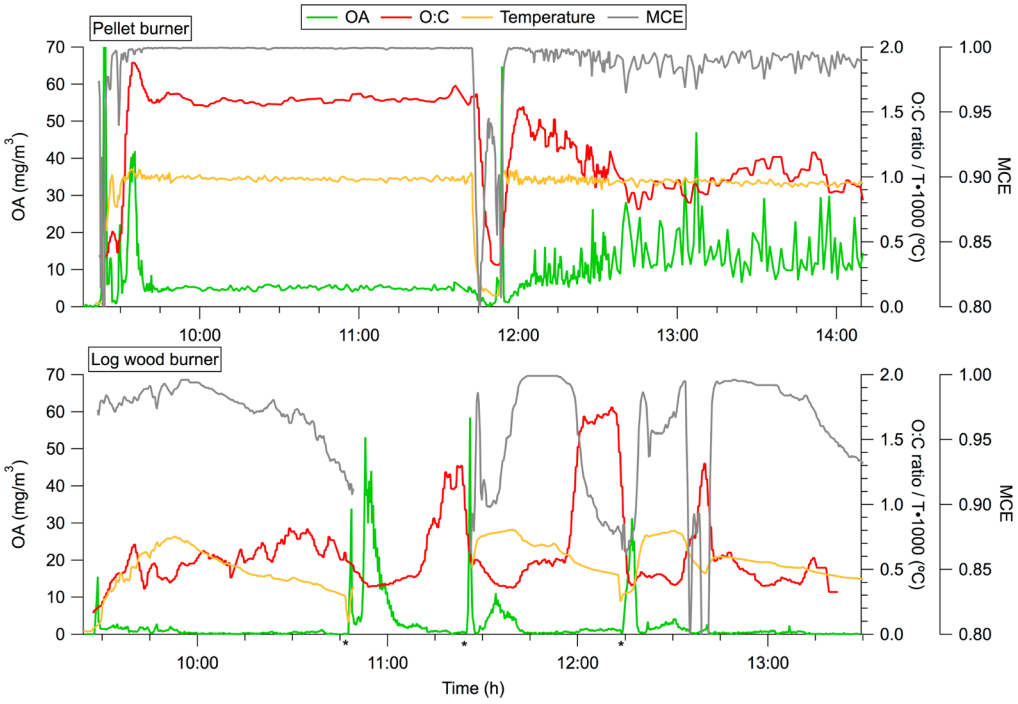

Figure 5. Temporal evolution of the OA and its O:C ratio (10 points (2.5−10 min) box smoothing) and MCE. The stars indicate the addition of wood logs to the fire. The temperature represents the temperature measured inside the combustion chamber.

the startup phase the gas phase HCs decreased rapidly to ~4.0 ppm carbon (ppm C), equaling approximately 3.4 mg/m^3 at an OM:OC ratio of 1.7 (found for the data in ref 10). This low level of gas phase HCs, compared to the 5.1 mg/m^3 OA, demonstrated the low SOA potential of pellet burners. This was also observed during smog chamber experiments where no SOA was formed during experiments on the emissions from an automatic pellet burner.[10]

The log wood burner emissions were dominated by BC except for the first minute after reloading the burner where the concentration of OA showed spikes generally preceding the spikes of BC. Low OM:BC ratios (<1) were also observed during other wood burning experiments [11] and during most of

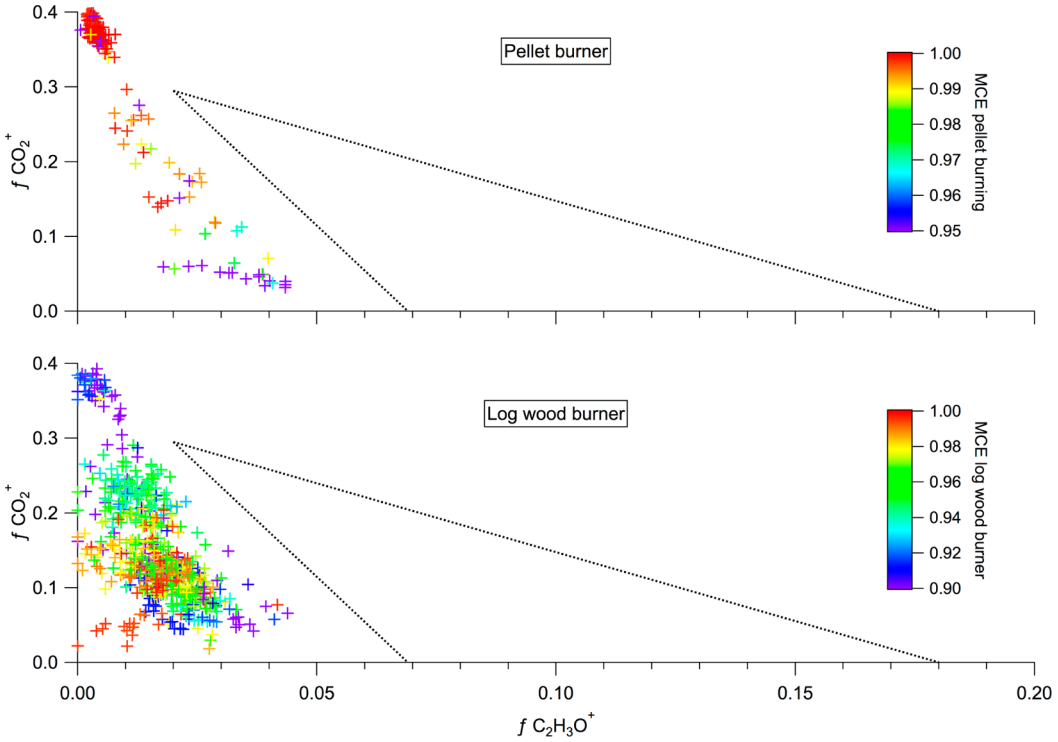

Figure 6. Fraction plot of $f\ CO_2^+$ vs $f\ C_2H_3O^+$. The triangular space found to accommodate the OOA component of ambient organic aerosol (Ng et al., 2010) is shown as well; all wood-burning emission points are found to the left of this atmospheric triangle. The data points are colored according to the MCE.

the smog chamber experiments described in Heringa et al.[10] These OM:BC ratios are at the lower edge of the range found by Grieshop et al. [9] and about an order of magnitude lower than the values reported for off-line measurements (ref 25 and reference therein). The high dilution factor used here is expected to lower the OM:BC ratio as a result of the change in partitioning of the SVOCs upon dilution.[26] Possible positive artifacts in the offline techniques, like adsorption, may also explain some of the differences. For the log wood burner the highest concentrations of gas phase HCs were observed directly after adding wood logs to the existing glow bed. However, even during the low emitting smoldering phase, HC concentrations were an order of magnitude higher than that measured for the pellet burner under stable burning conditions.

3.3. OA Characterization. Figure 4 shows the normalized high-resolution organic mass spectrum (MS) for the pellet burner and the log wood burner during different burning phases of the test cycle. The MS of the starting phase emissions of the pellet burner showed a significantly larger fraction of oxygen-containing ions than the starting phase spectrum of the log wood burner. The latter was governed more by the hydrocarbon series at m/z 41, 55, 69, 83 and m/z 43, 57, 71 typically assigned to cycloalkanes or alkenes ($C_nH_{2n-1}^+$) and normal or branched alkanes ($C_nH_{2n+1}^+$), respectively.[8,27,28] The MS recorded during stable burning conditions of the pellet burner showed high similarity to the MS of the log wood burner during the burnout phase. Both spectra were dominated by oxygenated ions with contributions of 90% and 92%, respectively. The ion $C_2H_4O_2^+$ at m/z 60, used as a marker for wood burning,[29] was most abundant during the startup phase of the pellet boiler (1.5%) followed by the flaming phase (0.6%) and the starting phase (0.4%) of the log wood burner. CO_2^+, an abundant fragment formed by thermal decomposition of acids and highly oxygenated compounds at the heater of the AMS, dominated the MS of the stable burning phase of the pellet burner, as well as the smoldering phase of the log wood burner. During poor burning conditions, the pellet burner MS was still dominated by CO_2^+ but showed a clear increase in the $C_nH_{2n-1}^+$ and $C_nH_{2n+1}^+$ series at m/z 41, 43, 55, 57, etc.

3.4. High-Resolution Analysis. The variability of the elemental O:C ratio during the experiment cycle is shown in Figure 5. The O:C ratio of the OA emitted during the startup of the pellet burner was ∼0.5 and increased after the first minutes to reach a plateau at 1.6 during the stable burning phase. When the air intake was restricted to achieve poor burning conditions, the O:C ratio decreased to ∼1. The O:C ratio of the OA produced by the log wood burner spanned a wide range during the different parts of the burning cycle. Generally, when the temperature inside the burning chamber was increasing or stable, an O:C ratio in the range 0.2−0.6 was found. At the end of the flaming phase of a batch, when the flames were dying, the temperature and MCE were decreasing, the O:C ratio increased up to 1.7. However, this increase was not observed at the same magnitude for all burnout phases during a burning cycle. A mass weighted average O:C ratio of 0.46 and 0.49 was found for the two log wood burner experiments shown in Figure 7. This shows that the low emitting periods with high O:C ratio do not have a major influence on the O:C ratio of the total emitted OA. The much higher O:C ratio of the pellet burner OA emissions, together with the higher salt fraction, makes it a more efficient cloud condensation nuclei. These differences should be acknowledged in models, especially when automated pellet burners gain popularity.

The fractions of two major ions in the mass spectrum, m/z 44 (CO_2^+) and m/z 43 (mostly $C_2H_3O^+$), are used as a

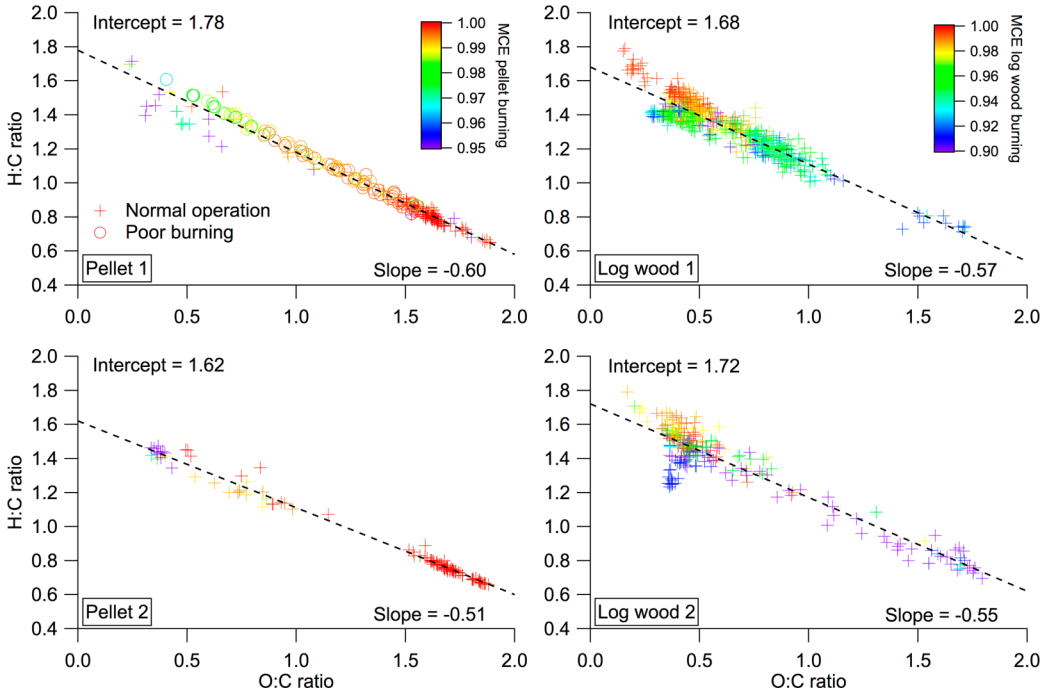

Figure 7. Van Krevelen diagrams for two pellet burner experiments (left) and two log wood burner measurements (right). The pellet burner data in the top panel is separated for normal operation and poor burning conditions. The data are colored by the MCE.

diagnostic tool to follow the aging of the oxidized OA (OOA) component in the atmosphere.[30] The f_{44} vs f_{43} plot was described to span a triangular space in which the OOA moves toward the apex during the aging process. Figure 6 shows the projection of the pellet burner data during normal operation and the complete log wood burner data as shown in Figures 3 and 5. All data points have a characteristic low fraction of $C_2H_3O^+$ for a given CO_2^+ fraction compared to ambient OOA, which is consistent with results from smog chamber experiments on wood burning emissions.[10,31] The data points start at low fCO_2^+ during the startup phase (or after adding a new batch) and move parallel to the triangle to higher fCO_2^+ when the burning continues. The pellet burner showed high fCO_2^+ at high MCE, whereas the log wood burner showed high fCO_2^+ during the smoldering phase characterized by a low MCE. The highest fCO_2^+ for the pellet and log wood burner OA exceeds the fraction found for ambient low volatility OOA (LV-OOA). However, as described above, these high fCO_2^+ particles from log wood burning are only responsible for a small fraction of the total emitted OA. A smog chamber experiment performed on wood burning OA with an O:C ratio of ~0.9 showed a decrease in OA during the first hours of photo-oxidation.[10] These highly oxygenated aerosols produced by the pellet burner might have a different lifetime due to differences in functionalization and fragmentation compared to OA from log wood burning. This would directly impact ambient PM levels originating from domestic wood burning and should be a topic of future research.

The Van Krevelen diagram (Figure 7) presents the relation of the H:C and O:C ratio for the wood-burning experiments shown before. Although the range in H:C and O:C ratio exceeds the range found for ambient data,[32,33] a linear relation was found throughout the whole range. In addition, emissions from both burners were found to behave very similarly in this plot with an average slope and intercept of −0.56 and 1.7, respectively.

On the basis of the linear relation between the O:C and H:C ratio, the average molecular formula of $C_xH_yO_z$ can be calculated for molecules with carbon number x. Since the number of nitrogen-containing compounds is very small (Figure 4), the average number of double bond equivalents (DBE) for compound $C_xH_yO_z$ can be calculated using the formula DBE = $1 + x - 0.5y$. A double bond equivalent can be a double bond between two carbon atoms, a carbon and an oxygen atom, or a ring structure. Organic molecules with higher DBE and thus (neglecting the ring structures) typically more double bonds are in general more reactive toward oxidants than organics with only C−C bonds. Information on the functionality of the organics is also interesting because the chemical, physical, and health-related properties are likely strongly linked to it. The two-dimensional space presented in Figure 8 shows the average number of DBE as a function of the O:C ratio and the number of carbon atoms. As these values are averaged over all compounds present in the OA, noninteger values are possible. The intercept of the Van Krevelen diagram indicates a hydrocarbon backbone (O:C = 0) with an average of

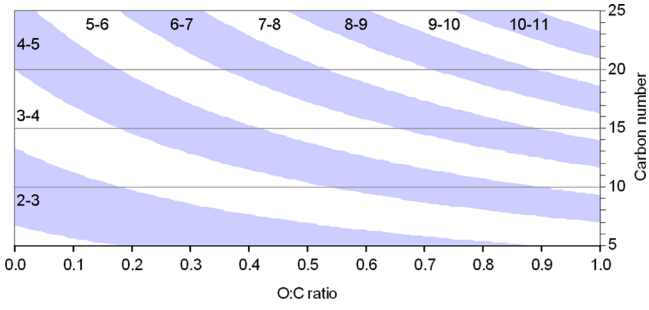

Figure 8. Average DBE as a function of the O:C ratio and the number of carbon atoms in the molecules. The numbers in the graph indicate the DBE range of the specific band.

dx.doi.org/10.1021/es301654w | Environ. Sci. Technol. 2012, 46, 11418−11425

2.5 double bond equivalents (DBE) for a 10 carbon molecule or 4 DBE for a 20 carbon molecule. The DBE for the oxygen-containing molecule $C_xH_yO_z$ follows the formula $0.15x + 0.28x \cdot O{:}C + 1$, indicating that for a constant number of carbons atoms the DBE increases with increasing O:C ratio. Additionally, DBE is increasing at any O:C ratio with increasing carbon number where the increase at higher O:C ratios is steeper than that at lower O:C ratios. Additional information on the molecular weight, e.g., from a soft ionization mass spectrometry method like chemical ionization, would be useful to narrow the range of the predicted DBE and retrieve more accurate data information about the average structural features of the OA.

■ ASSOCIATED CONTENT

Supporting Information

This material is available free of charge via the Internet at http://pubs.acs.org.

■ AUTHOR INFORMATION

Corresponding Author

*Phone: +41 56 310 4202; e-mail: andre.prevot@psi.ch.

Present Addresses

[⊥]Department of Civil, Architectural and Environmental Engineering, Drexel University, Philadelphia, Pennsylvania, United States.

[#]Italian National Agency for New Technologies, Energy and Sustainable Economic Development (ENEA), UTAPRAD-DIM, Via E. Fermi 45, 00044 Frascati, Italy.

[¶]Labor Veritas AG, 8002 Zurich, Switzerland.

[▲]University of Applied Sciences, Northwestern Switzerland, 5210 Windisch, Switzerland.

Notes

The authors declare no competing financial interest.

■ ACKNOWLEDGMENTS

This work was supported by the IMBALANCE project of the Competence Center Environment and Sustainability of the ETH Domain (CCES), the Bundesamt für Umwelt (BAFU), the Bundesamt für Energie (BFE), as well as the Swiss National Science Foundation. P.F.D. is grateful for the postdoctoral support from the US-NSF (IRFP# 0701013).

■ REFERENCES

(1) Lanz, V. A.; Prevot, A. S. H.; Alfarra, M. R.; Weimer, S.; Mohr, C.; DeCarlo, P. F.; Gianini, M. F. D.; Hueglin, C.; Schneider, J.; Favez, O.; D'Anna, B.; George, C.; Baltensperger, U. Characterization of aerosol chemical composition with aerosol mass spectrometry in Central Europe: an overview. *Atmos. Chem. Phys.* **2010**, *10* (21), 10453−10471.

(2) Sandradewi, J.; Prevot, A. S. H.; Szidat, S.; Perron, N.; Alfarra, M. R.; Lanz, V. A.; Weingartner, E.; Baltensperger, U. Using aerosol light absorption measurements for the quantitative determination of wood burning and traffic emission contributions to particulate matter. *Environ. Sci. Technol.* **2008**, *42* (9), 3316−3323.

(3) Szidat, S.; Prevot, A. S. H.; Sandradewi, J.; Alfarra, M. R.; Synal, H. A.; Wacker, L.; Baltensperger, U. Dominant impact of residential wood burning on particulate matter in Alpine valleys during winter. *Geophys. Res. Lett.* **2007**, *34* (5), L05820.

(4) McDonald, J. D.; Zielinska, B.; Fujita, E. M.; Sagebiel, J. C.; Chow, J. C.; Watson, J. G. Fine particle and gaseous emission rates from residential wood combustion. *Environ. Sci. Technol.* **2000**, *34* (11), 2080−2091.

(5) Schauer, J. J.; Kleeman, M. J.; Cass, G. R.; Simoneit, B. R. T. Measurement of emissions from air pollution sources. 3. C_1-C_{29} organic compounds from fireplace combustion of wood. *Environ. Sci. Technol.* **2001**, *35* (9), 1716−1728.

(6) Chen, Y.; Roden, C. A.; Bond, T. C. Characterizing biofuel combustion with patterns of real-time emission data (PaRTED). *Environ. Sci. Technol.* **2012**, *46* (11), 6110−6117.

(7) Hays, M. D.; Gullett, B.; King, C.; Robinson, J.; Preston, W.; Touati, A. Characterization of carbonaceous aerosols emitted from outdoor wood boilers. *Energy Fuels* **2011**, *25* (12), 5632−5638.

(8) Weimer, S.; Alfarra, M. R.; Schreiber, D.; Mohr, M.; Prévôt, A. S. H.; Baltensperger, U. Organic aerosol mass spectral signatures from wood-burning emissions: Influence of burning conditions and wood type. *J. Geophys. Res.* **2008**, *113*, D10304.

(9) Grieshop, A. P.; Logue, J. M.; Donahue, N. M.; Robinson, A. L. Laboratory investigation of photochemical oxidation of organic aerosol from wood fires 1: measurement and simulation of organic aerosol evolution. *Atmos. Chem. Phys.* **2009**, *9* (4), 1263−1277.

(10) Heringa, M. F.; DeCarlo, P. F.; Chirico, R.; Tritscher, T.; Dommen, J.; Weingartner, E.; Richter, R.; Wehrle, G.; Prevot, A. S. H.; Baltensperger, U. Investigations of primary and secondary particulate matter of different wood combustion appliances with a high-resolution time-of-flight aerosol mass spectrometer. *Atmos. Chem. Phys.* **2011**, *11* (12), 5945−5957.

(11) Oser, M.; Nussbaumer, Th.; Müller, P.; Mohr, M.; Figi, R., Mechanisms of particle formation in biomass combustion. *Proceedings Second World Biomass Conference*, 10−14 May 2004, Rome, ETA Florence and WIP Munich, ISBN 88-89407-04-2, 1246-1249.

(12) Bell, M. L.; Davis, D. L. Reassessment of the lethal London fog of 1952: Novel indicators of acute and chronic consequences of acute exposure to air pollution. *Environ. Health Persp.* **2001**, *109*, 389−394.

(13) Laden, F.; Schwartz, J.; Speizer, F. E.; Dockery, D. W. Reduction in fine particulate air pollution and mortality - Extended follow-up of the Harvard six cities study. *Am. J. Resp. Crit. Care* **2006**, *173* (6), 667−672.

(14) Pope, C. A.; Burnett, R. T.; Thun, M. J.; Calle, E. E.; Krewski, D.; Ito, K.; Thurston, G. D. Lung cancer, cardiopulmonary mortality, and long-term exposure to fine particulate air pollution. *J. Am. Med. Assoc.* **2002**, *287* (9), 1132−1141.

(15) Miljevic, B.; Heringa, M. F.; Keller, A.; Meyer, N. K.; Good, J.; Lauber, A.; Decarlo, P. F.; Fairfull-Smith, K. E.; Nussbaumer, T.; Burtscher, H.; Prevot, A. S.; Baltensperger, U.; Bottle, S. E.; Ristovski, Z. D. Oxidative potential of logwood and pellet burning particles assessed by a novel profluorescent nitroxide probe. *Environ. Sci. Technol.* **2010**, *44* (17), 6601−7.

(16) Good, J.; Nussbaumer, T. Prüfverfahren für die Startphase auf der Basis von EN 303-5: 1. Stückholzkessel , 2010.

(17) Nussbaumer, T.; Czasch, C.; Klippel, N.; Johansson, L.; Tullin, C. *Particulate emissions from biomass combustion in IEA countries; Survey on measurements and emission factors*; International Energy Agency (IEA) Bioenergy Task 32 and Swiss Federal Office of Energy (SFOE): Zürich, 2008.

(18) DeCarlo, P. F.; Kimmel, J. R.; Trimborn, A.; Northway, M. J.; Jayne, J. T.; Aiken, A. C.; Gonin, M.; Fuhrer, K.; Horvath, T.; Docherty, K. S.; Worsnop, D. R.; Jimenez, J. L. Field-deployable, high-resolution, time-of-flight aerosol mass spectrometer. *Anal. Chem.* **2006**, *78* (24), 8281−8289.

(19) Allan, J. D.; Delia, A. E.; Coe, H.; Bower, K. N.; Alfarra, M. R.; Jimenez, J. L.; Middlebrook, A. M.; Drewnick, F.; Onasch, T. B.; Canagaratna, M. R.; Jayne, J. T.; Worsnop, D. R. A generalised method for the extraction of chemically resolved mass spectra from Aerodyne aerosol mass spectrometer data. *J. Aerosol Sci.* **2004**, *35* (7), 909−922.

(20) Aiken, A. C.; DeCarlo, P. F.; Jimenez, J. L. Elemental analysis of organic species with electron ionization high-resolution mass spectrometry. *Anal. Chem.* **2007**, *79* (21), 8350−8358.

(21) Aiken, A. C.; DeCarlo, P. F.; Kroll, J. H.; Worsnop, D. R.; Huffman, J. A.; Docherty, K. S.; Ulbrich, I. M.; Mohr, C.; Kimmel, J. R.; Sueper, D.; Sun, Y.; Zhang, Q.; Trimborn, A.; Northway, M.; Ziemann, P. J.; Canagaratna, M. R.; Onasch, T. B.; Alfarra, M. R.; Prevot, A. S. H.; Dommen, J.; Duplissy, J.; Metzger, A.; Baltensperger, U.; Jimenez, J. L. O/C and OM/OC ratios of primary, secondary, and

ambient organic aerosols with high-resolution time-of-flight aerosol mass spectrometry. *Environ. Sci. Technol.* **2008**, *42* (12), 4478−4485.
(22) Petzold, A.; Kramer, H.; Schonlinner, M. Continuous measurement of atmospheric black carbon using a multi-angle absorption photometer. *Environ. Sci. Pollut. Res.* **2002**, 78−82.
(23) Fine, P. M.; Cass, G. R.; Simoneit, B. R. T. Chemical characterization of fine particle emissions from the wood stove combustion of prevalent United States tree species. *Environ. Eng. Sci.* **2004**, *21* (6), 705−721.
(24) Fierz, M.; Burtscher, H.; Steigmeier, P.; Kasper, M. Field measurement of particle size and number concentration with the diffusion size classifier (Disc). *SAE Technical Paper* **2008**, 2008−01−1179, DOI: 10.4271/2008-01-1179.
(25) Szidat, S.; Jenk, T. M.; Synal, H.-A.; Kalberer, M.; Wacker, L.; Hajdas, I.; Kasper-Giebl, A.; Baltensperger, U. Contributions of fossil fuel, biomass-burning, and biogenic emissions to carbonaceous aerosols in Zurich as traced by ^{14}C. *J. Geophys. Res.* **2006**, *111*, D07206.
(26) Donahue, N. M.; Robinson, A. L.; Stanier, C. O.; Pandis, S. N. Coupled partitioning, dilution, and chemical aging of semivolatile organics. *Environ. Sci. Technol.* **2006**, *40* (8), 2635−2643.
(27) Alfarra, M. R.; Coe, H.; Allan, J. D.; Bower, K. N.; Boudries, H.; Canagaratna, M. R.; Jimenez, J. L.; Jayne, J. T.; Garforth, A. A.; Li, S. M.; Worsnop, D. R. Characterization of urban and rural organic particulate in the lower Fraser valley using two Aerodyne aerosol mass spectrometers. *Atmos. Environ.* **2004**, *38* (34), 5745−5758.
(28) Canagaratna, M. R.; Jayne, J. T.; Ghertner, D. A.; Herndon, S.; Shi, Q.; Jimenez, J. L.; Silva, P. J.; Williams, P.; Lanni, T.; Drewnick, F.; Demerjian, K. L.; Kolb, C. E.; Worsnop, D. R. Chase studies of particulate emissions from in-use New York City vehicles. *Aerosol. Sci. Technol.* **2004**, *38* (6), 555−573.
(29) Alfarra, M. R.; Prevot, A. S. H.; Szidat, S.; Sandradewi, J.; Weimer, S.; Lanz, V. A.; Schreiber, D.; Mohr, M.; Baltensperger, U. Identification of the mass spectral signature of organic aerosols from wood burning emissions. *Environ. Sci. Technol.* **2007**, *41* (16), 5770−5777.
(30) Ng, N. L.; Canagaratna, M. R.; Zhang, Q.; Jimenez, J. L.; Tian, J.; Ulbrich, I. M.; Kroll, J. H.; Docherty, K. S.; Chhabra, P. S.; Bahreini, R.; Murphy, S. M.; Seinfeld, J. H.; Hildebrandt, L.; Donahue, N. M.; DeCarlo, P. F.; Lanz, V. A.; Prevot, A. S. H.; Dinar, E.; Rudich, Y.; Worsnop, D. R. Organic aerosol components observed in Northern Hemispheric datasets from aerosol mass spectrometry. *Atmos. Chem. Phys.* **2010**, *10* (10), 4625−4641.
(31) Heringa, M. F.; DeCarlo, P. F.; Chirico, R.; Tritscher, T.; Clairotte, M.; Mohr, C.; Crippa, M.; Slowik, J. G.; Pfaffenberger, L.; Dommen, J.; Weingartner, E.; Prevot, A. S. H.; Baltensperger, U. A new method to discriminate secondary organic aerosols from different sources using high-resolution aerosol mass spectra. *Atmos. Chem. Phys.* **2012**, *12* (4), 2189−2203.
(32) Heald, C. L.; Kroll, J. H.; Jimenez, J. L.; Docherty, K. S.; DeCarlo, P. F.; Aiken, A. C.; Chen, Q.; Martin, S. T.; Farmer, D. K.; Artaxo, P. A simplified description of the evolution of organic aerosol composition in the atmosphere. *Geophys. Res. Lett.* **2010**, *37*, L08803.
(33) Jimenez, J. L.; Canagaratna, M. R.; Donahue, N. M.; Prevot, A. S. H.; Zhang, Q.; Kroll, J. H.; DeCarlo, P. F.; Allan, J. D.; Coe, H.; Ng, N. L.; Aiken, A. C.; Docherty, K. S.; Ulbrich, I. M.; Grieshop, A. P.; Robinson, A. L.; Duplissy, J.; Smith, J. D.; Wilson, K. R.; Lanz, V. A.; Hueglin, C.; Sun, Y. L.; Tian, J.; Laaksonen, A.; Raatikainen, T.; Rautiainen, J.; Vaattovaara, P.; Ehn, M.; Kulmala, M.; Tomlinson, J. M.; Collins, D. R.; Cubison, M. J.; Dunlea, E. J.; Huffman, J. A.; Onasch, T. B.; Alfarra, M. R.; Williams, P. I.; Bower, K.; Kondo, Y.; Schneider, J.; Drewnick, F.; Borrmann, S.; Weimer, S.; Demerjian, K.; Salcedo, D.; Cottrell, L.; Griffin, R.; Takami, A.; Miyoshi, T.; Hatakeyama, S.; Shimono, A.; Sun, J. Y.; Zhang, Y. M.; Dzepina, K.; Kimmel, J. R.; Sueper, D.; Jayne, J. T.; Herndon, S. C.; Trimborn, A. M.; Williams, L. R.; Wood, E. C.; Middlebrook, A. M.; Kolb, C. E.; Baltensperger, U.; Worsnop, D. R. Evolution of organic aerosols in the atmosphere. *Science* **2009**, *326* (5959), 1525−1529.